

Intracavity absorption spectroscopy of formaldehyde from 6230 to 6420 cm^{-1}

Peter Fjodorow¹ · Ortwin Hellmig² · Valery M. Baev² · Howard B. Levinsky³ · Anatoli V. Mokhov³

Received: 31 January 2017 / Accepted: 6 April 2017 / Published online: 18 April 2017
© Springer-Verlag Berlin Heidelberg 2017

Abstract We apply intracavity absorption spectroscopy for measurements of the absorption spectrum of formaldehyde, CH_2O , from 6230 to 6420 cm^{-1} , of which only a small fraction (6351–6362 cm^{-1}) has been recorded elsewhere. The measurements are performed in the cavity of a broadband Er^{3+} -doped fiber laser, with a sensitivity corresponding to the effective absorption path length of 45 m and a spectral resolution of 0.1 cm^{-1} . The noise-equivalent detection limit of CH_2O achieved with the strongest absorption line at 6252.64 cm^{-1} is estimated to be 5 ppm. High tolerance to broadband losses and the accessible time resolution of 50 μs make it possible to apply this detection system for time-resolved monitoring of CH_2O together with other molecules in harsh combustion environments, e.g., in combustion engines.

1 Introduction

Formaldehyde (CH_2O) occurs in the Earth atmosphere, interstellar space, living organisms, and as one of the important intermediate components in hydrocarbon

oxidation. In combustion processes, during ignition, part of the fuel is converted to CH_2O before substantial heat release. The complex chemical interaction of CH_2O with oxidizer, fuel, and other intermediates determines the ignition delay time, i.e., the time between bringing the fuel/oxidizer mixture into ignition conditions (usually by compression) and its conversion into combustion products. Fundamental understanding of the chemical and physical processes responsible for ignition is essential for efficient and safe operation of combustion equipment. Usually, experimental studies of ignition processes are performed by measuring ignition delay times. However, the amount of detailed information derived from ignition delay times is very limited, and consequently, time-resolved studies of the ignition process are required for understanding the underlying physical/chemical processes. The comparison of measured temporal profiles of intermediate species (e.g., CH_2O) with those calculated using detailed combustion mechanisms, is capable of providing insights into ignition processes and to verify and/or improve theoretical models. Laser-diagnostic techniques with high sensitivity and high sampling rates are required for this purpose. Although laser diagnostics of CH_2O in combustion environments are relatively well established, none of the techniques usually applied is capable of fully satisfying the requirements posed by the harsh environment, the low species concentration, and the fast reaction rates.

One of the most established laser-based methods for measuring CH_2O in combustion environments is laser-induced fluorescence (LIF). It provides high sensitivity, together with high temporal and spatial resolution. LIF was successfully implemented for combustion diagnostics of CH_2O in laminar and turbulent flames, flow reactors, and engines [1–3]. Unfortunately, this method is difficult to apply for quantitative diagnostics because of substantial

This article is part of the topical collection “Field Laser Applications in Industry and Research” guest edited by Francesco D’Amato, Erik Kerstel, and Alan Fried.

✉ Valery M. Baev
baev@physnet.uni-hamburg.de

¹ Institute for Combustion and Gas Dynamics, University of Duisburg-Essen, Duisburg, Germany

² Institute of Laser Physics, University of Hamburg, Hamburg, Germany

³ Energy and Sustainability Research Institute, University of Groningen, Groningen, The Netherlands

background from other intermediates and limited knowledge about collisional processes, which determine the quantum yield of fluorescence. Furthermore, despite of the availability of powerful high-repetition rate UV lasers, LIF measurements with acceptable signal-to-noise ratio for sampling rates above 10 kHz are currently not feasible.

Absorption measurements can potentially provide high sensitivity at high sampling rates. Formaldehyde has been measured using direct absorption in shock tubes [4, 5] and, recently, in UV and mid-infrared (MIR) spectral regions [6]. However, while these studies showed high potential for the implementation of absorption spectroscopy in high-temperature environments, the reported sensitivity of the direct one-pass absorption spectroscopy is not sufficient for the detection of CH_2O concentrations below 100 ppm, which are expected in the initial stages of the ignition process. The implementation of multipass configurations is more promising for this purpose, because sufficient sensitivity can be achieved, even on weak absorption features. In fact, the most sensitive absorption techniques are currently based on a multipass setup, most often involving a passive high-finesse cavity.

One of these techniques used for CH_2O detection is cavity-enhanced absorption spectroscopy (CEAS), as reported in [7]. These authors observed a very dense CH_2O spectrum in the spectral region of $6547\text{--}6804\text{ cm}^{-1}$ ($1.469\text{--}1.527\text{ }\mu\text{m}$). Zhao et al. [8] measured the absorption spectrum of CH_2O around $1.573\text{ }\mu\text{m}$ ($6351.3\text{--}6362\text{ cm}^{-1}$) using off-axis integrated cavity output spectroscopy (OA-ICOS). This latter spectral region is of particular interest, because it can be accessed with a widely tunable erbium laser. However, these techniques, and most of the approaches involving passive-cavity configurations, are not well suited for measurements in harsh combustion environments, because of their susceptibility to broadband losses.

Another way of exploiting the multipass approach involves an active cavity, i.e., the sample is introduced directly into the laser resonator. In this technique, intracavity absorption spectroscopy (ICAS) [9], the light also travels many roundtrips through the absorber, ensuring a long effective absorption path, L_{eff} . However, in contrast to passive-cavity configurations, the broadband laser gain effectively compensates the broadband cavity losses that are caused by density fluctuations, broadband absorption, or light scattering, for example. On the other hand, narrow-line absorption appears as absorption lines in the emission spectrum of the laser [9, 10]. The absorption signal is measured as the relative change of the spectral power density due to absorption. Consequently, fluctuations in the total power of the laser do not influence the sensitivity or accuracy of ICAS measurements. These features of ICAS are especially advantageous for measurements in hostile environments.

This technique allows ultra-sensitive measurements with up to 8 orders of magnitude larger effective

absorption path lengths compared to single-pass absorption [11]. Furthermore, since broadband laser sources are exploited for ICAS, this technique enables simultaneous concentration measurements of different molecular species [9, 12], investigation of chemical reactions and their rates [13, 14], and simultaneous determination of temperature, pressure, and concentrations of gaseous samples [12, 15, 16]. Moreover, ICAS is capable of monitoring single transient processes with microsecond time resolution [17] and to operate in hostile environments [10]. To our knowledge, ICAS has yet not been applied to the detection of CH_2O .

In this work, we present our measurements of CH_2O using an ICAS setup based on an Er^{3+} -doped fiber laser operating in the spectral region from 6230 to 6420 cm^{-1} . Since ICAS, due to its high time resolution, high sensitivity, and high tolerance to broadband losses, has proven its potential for multicomponent measurements in demanding environments, we propose this technique as a versatile tool for diagnostics applications in nonstationary combustion environments such as rapid compression machines (RCM) and combustion engines. It should be noted that sensitive measurements of other important molecules, such as CO , CO_2 , OH , H_2O , H_2S , NH_3 , C_2H_2 , and HCN , can be simultaneously performed with the same laser system [12].

2 Experimental setup

The experimental configuration used for the current work is shown in Fig. 1. As a broadband laser source, we use a compact, home-made Er^{3+} -doped fiber laser. The most

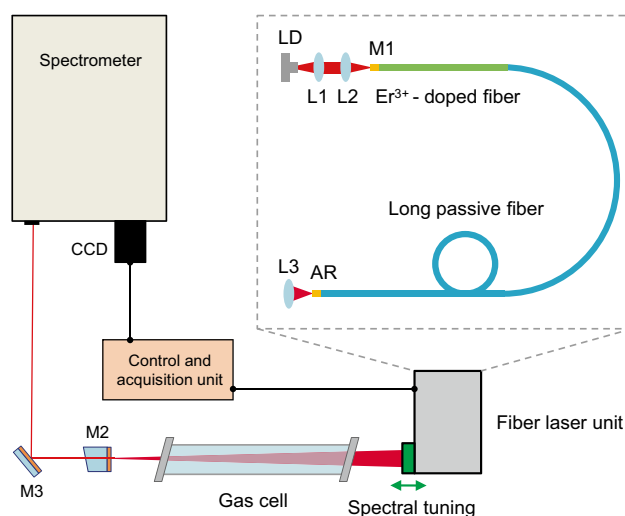


Fig. 1 Experimental setup

important components of the laser are depicted in the dashed area in Fig. 1. The active material of the laser is a 2-m Er^{3+} -doped optical fiber (Liekki, Er16-8/125). For the purpose of noise reduction in single spectra [16, 17], a 50 m piece of passive fiber (Nufern, 1550B-HP) is spliced to the active fiber and the whole fiber is coiled to a diameter of 6 cm. As a pump source, we use a laser diode (LD) emitting at 980 nm (Axcel Photonics, M9-980-0300-S50), with a maximum power of 300 mW. All of the components shown in the dashed area of Fig. 1 are incorporated into a small box.

The pump light is collimated with the lens L1 and focused into the fiber core by the lens L2. The fiber coating, M1, is a home-made dielectric layer system, providing high transmission for the pump light and high reflectivity for the laser light around 1.6 μm . This coating acts as the end mirror of the laser cavity. To avoid parasitic interferometric fringes, the second end of the fiber and all other optical elements inside the laser cavity (i.e., between M1 and M2) are anti-reflection coated (AR). The lens L3 focuses the light coming from the fiber onto the plane output mirror M2 ($R \approx 98\%$) and then back into the fiber. Translation of the lens L3 along the optical axis leads to wavelength-dependent changes in the coupling efficiency, due to chromatic aberration. The interplay between this added loss and the gain profile of the active fiber determines the position of the emission spectrum of the fiber laser, thus providing a very simple and effective method for a broadband spectral tuning.

A sample cell ($L = 25$ cm) is placed inside the laser cavity between L3 and M2. The total optical length of the cavity is calculated as $L_{\text{opt}} = \sum L_i n_i$, where L_i are the geometrical lengths of optical components in the laser cavity and n_i are their refractive indices. The most important contributions to L_{opt} come from the optical fiber (52 m, $n = 1.47$) and from the open part of the cavity (0.6 m, $n = 1$). Here-with, the total optical length of the laser cavity results in $L_{\text{opt}} = 77$ m, while the filling factor of the laser cavity with the absorber, $\beta = LL_{\text{opt}}$, amounts to 0.3%.

The laser light is coupled to a spectrometer (Jobin-Yvon, THR 1000, grating with 300 groves/mm) and analyzed with a CCD line scan camera (Goodrich Sensors Unlimited, SU-LDH, 1024 pixels). The time window for spectral detection can be set to the required value by an external function generator. The total spectral resolution of the recording system is $\Delta\nu = 0.1 \text{ cm}^{-1}$.

The “control and acquisition unit” in Fig. 1 represents the associated electronic equipment (e.g., laser diode driver, photodiodes, oscilloscope, computer with LabVIEW, and function generator). A two-channel function generator provides synchronized signals to control the pump power of the laser and the recording window of the CCD.

The sensitivity of absorption measurements is controlled by modulating the pump power. In general, the effective absorption path length L_{eff} of ICAS is determined by the laser pulse duration, t , as $L_{\text{eff}} = ct$ [9], with c being the velocity of light. This feature can be used for the adjustment of sensitivity to the required level. However, it should be noted that higher sensitivity results in a reduced time resolution, which is determined by the laser pulse duration. In our experiment, the width of the pump pulses is chosen, such that only the first pulse of relaxation oscillations of the Er^{3+} -doped fiber laser with $t = 50 \mu\text{s}$ is generated [18]. It results in the effective absorption path length of $L_{\text{eff}} = 15$ km. Taking into account the filling factor of the cavity with the absorber, $\beta = 0.003$, the effective absorption path length reduces to $L_{\text{eff},\beta} = 45$ m.

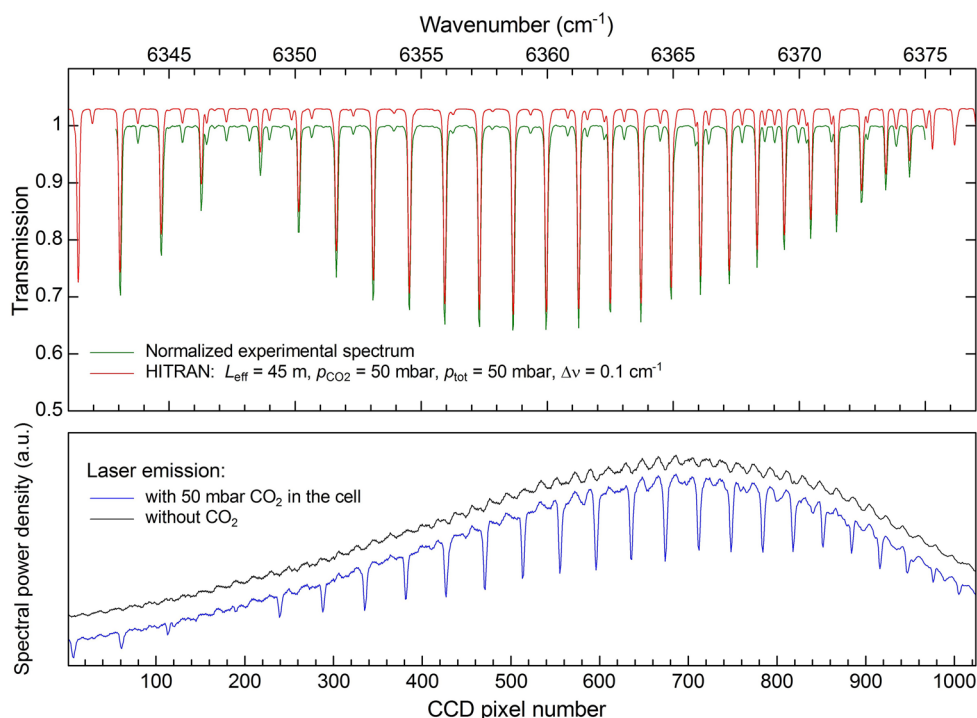
If necessary, the sensitivity of measurements can be increased using longer laser pulses. For our Er^{3+} -doped fiber laser with the spectral saturation time of about 500 μs the maximum sensitivity corresponds to the effective absorption length $L_{\text{eff},\beta} \approx 450$ m. Further enhancement of the sensitivity can be achieved by increasing the filling factor of the cavity with the absorber and using other lasers with a larger value of the spectral saturation time, e.g., an Er^{3+} -doped crystal laser. Solid-state lasers usually have larger spectral saturation times than fiber lasers due to lower values of Rayleigh scattering in the active medium [9]. However, fiber lasers have much lower laser thresholds and can be easier applied to the measurements in hostile environments with up to 50% added cavity losses.

3 Spectral calibration

Wavelength calibration of the spectra recorded with our CCD camera is performed by measuring well-known absorption spectra, e.g., available in the HITRAN database [19]. For this purpose, depending on the spectral position, we have selected CO or CO_2 molecules and fit their normalized absorption spectra to the spectra calculated from the HITRAN database. Besides the spectral calibration, this procedure assesses the estimated sensitivity using the effective absorption path length, L_{eff} , as a fit parameter for HITRAN calculations.

Figure 2 shows the calibration performed with the intracavity cell filled with 50 mbar of CO_2 . The bottom part of Fig. 2 shows the emission spectrum of the laser with (blue) and without (black) CO_2 in the cell, recorded without spectral tuning. The spectral width of the laser is about 40 cm^{-1} and includes many absorption lines of CO_2 . The emission spectra of the laser exhibit a reproducible background structure, which is caused by etalon fringes due to residual reflections from various optical components in the laser

Fig. 2 Bottom emission spectra of the Er^{3+} -doped fiber laser with (blue) and without (black) CO_2 in the absorption cell. Top normalized experimental spectrum (green) superimposed with a calculated spectrum (red) using the HITRAN database. The spectrum without CO_2 (black) and the calculated spectrum (red) are shifted along the vertical axis for better comparison



cavity and from possible imperfections in the fiber. This background structure has been eliminated by dividing the spectrum recorded with a sample in the laser cavity by the spectrum recorded without the sample. The resulting normalized spectrum (Fig. 2, top, green) shows an intracavity absorption spectrum of CO_2 without background structure. The residual spectral noise amounts only 0.05% (RMS) in the center of laser emission spectrum. The noise-equivalent detection limit of CO_2 in this operational mode of the laser is about 50 ppm. The spectral calibration is performed by fitting the absorption spectrum by the spectrum simulated with a HITRAN data base including absorbing molecules. If such calibration involves many absorption lines, e.g., 25 in the case of Fig. 2, the overall accuracy of the fit is of the order of 0.001 cm^{-1} .

As can be seen from Fig. 2 (top), there is an excellent agreement between the experimental and the calculated spectra, including all strong and weak absorption features. This demonstrates the capability of ICAS to deliver very accurate and sensitive spectroscopic data.

4 Production of formaldehyde by pyrolysis of polyoxymethylene (POM) and experimental results of ICAS in a CH_2O gas mixture

Spectral measurements of CH_2O are more complicated, since gaseous CH_2O is not commercially available in significant concentrations, due to its polymerization into paraformaldehyde [20]. Therefore, we have produced

fresh CH_2O in our laboratory just prior to measurement by the pyrolysis of the polymer polyoxymethylene (POM). For this purpose, small pieces of POM are heated in a glass tube placed inside an oven at the temperature of about 750 K. Under these conditions, POM is known to decompose into more than 50 gaseous constituents, with the main product CH_2O , being roughly 95% of all compounds formed [21]; this provides a suitable gas mixture for spectroscopic measurements of CH_2O . The gas mixture is collected in a Tedlar gas bag by introducing a small helium flow on one side of the glass tube and is immediately transferred into the evacuated sample cell. The problem of polymerization of CH_2O is solved by heating the absorption cell to around 350 K. Without this heating, the cell walls become successively covered by a white film of paraformaldehyde and, as a consequence, a continuous decrease in line strengths of CH_2O in the ICAS spectra is observed. However, upon cell heating—the paraformaldehyde decomposes again into CH_2O and the absorption lines recover their original strengths. The concentration of the CH_2O in the gas mixture is estimated using wet-chemical means to be 1%. This was assessed by quantitative dissolution of CH_2O in water, as a so-called impingement fluid, and subsequent derivatization using acetylacetone, followed by colorimetric determination of the concentration using a benchtop spectrophotometer (Hach Lange, DR2800). The premeasured reagents used in this process were obtained commercially (Hach Lange, LCK 325). The accuracy of this calibration method is 10%, which is sufficient for the purpose of this study.

After these preparatory steps, we have measured the spectrum of CH_2O in the entire emission range of our laser from 6230 to 6420 cm^{-1} , achieved by successive spectral tuning. The accessible spectral region is covered by nine overlapping emission spectra of the Er^{3+} -doped fiber laser. Subsequently, these spectra are normalized by the laser emission spectra recorded without CH_2O and then combined together in the full spectrum accessible with our laser, as shown in Fig. 3.

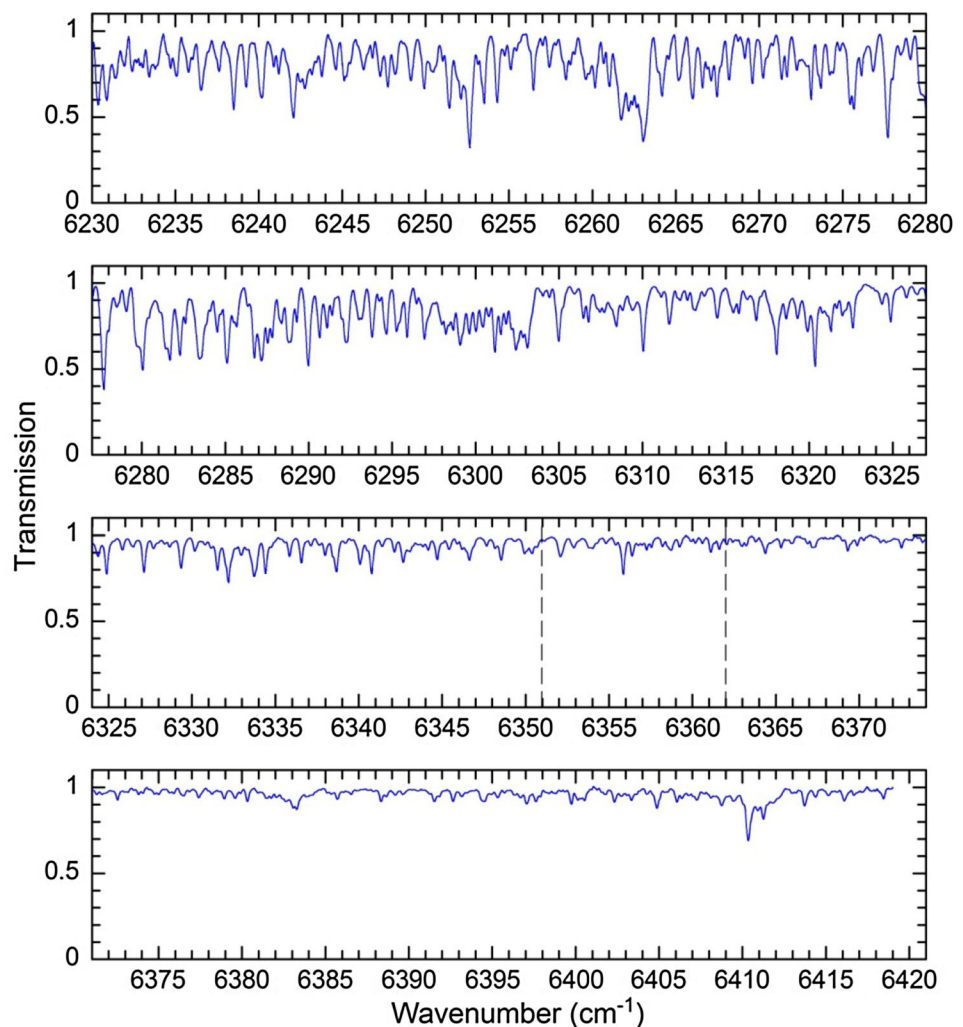
Figure 3 shows the absorption spectrum obtained for 1% CH_2O in air at pressure of 1 bar and temperature of 350 K, recorded as described above, with a sensitivity corresponding to $L_{\text{eff}} = 45$ m and a spectral resolution of 0.1 cm^{-1} . The combined absorption spectrum of CH_2O is presented in four diagrams. Only a small segment of this spectrum (between the dashed lines) has been recorded previously [8]. A comparison of our results with these earlier measurements confirms that all the observed lines in the range from 6351 to 6362 cm^{-1} originate from CH_2O absorption.

This observation demonstrates that the production of CH_2O by pyrolysis of POM is adequate for spectroscopic measurements.

The strongest absorption line of CH_2O recorded in our experiment is located at 6252.64 cm^{-1} . Its absorption signal is five times larger than the strongest absorption observed earlier [8] and enables us to achieve higher concentration sensitivity to CH_2O . The resulting noise-equivalent detection limit of CH_2O , obtained by extrapolating the absorption signal of this line to the noise level of 0.05% (RMS), is about 5 ppm. If necessary, a detection limit below 1 ppm can be achieved with longer laser pulses, however, with the reduced time resolution for single-shot measurements mentioned above.

Based on the spectroscopic results obtained here, it is illustrative to discuss the implementation of the ICAS technique for time-resolved diagnostics of elementary processes leading to ignition. As an example, we take the expected temporal profiles of the temperature and

Fig. 3 Absorption spectrum of CH_2O ($p_{\text{CH}_2\text{O}} = 1\%$, $p_{\text{tot}} = 1$ bar, $T = 350$ K) recorded inside the cavity of an Er^{3+} -doped fiber laser. The combined absorption spectrum of CH_2O is presented in four diagrams. The spectral region between the dashed lines has been recorded earlier [8]



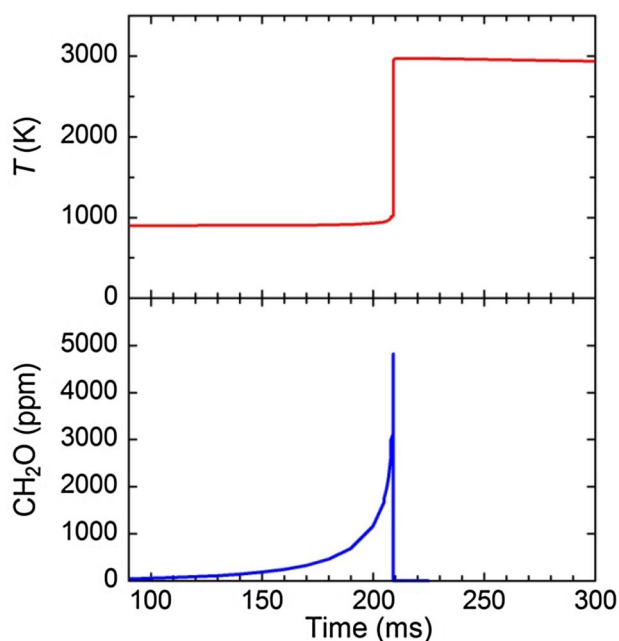


Fig. 4 Calculated temporal profiles of temperature (*red*) and concentration of CH_2O (*blue*) during ignition of a stoichiometric CH_4/air mixture held at constant volume at the initial compression conditions of $p_c = 30$ bar and $T_c = 900$ K

CH_2O concentration obtained by solving the governing equations for a stoichiometric CH_4/air mixture held at constant volume at the initial compression conditions of $p_c = 30$ bar and $T_c = 900$ K, using the code from the Cantera suite [22] with the GRI-Mech 3.0 chemical mechanism [23], which are shown in Fig. 4.

As can be seen, up to the ignition moment at 210 ms after the compression, the temperature remains constant at roughly 900 K, while the fraction of CH_2O is steadily growing up to a maximum concentration of about 5000 ppm. The growth of CH_2O is due to complex interplay of multiple reactions of production and consumption of radicals that ultimately determines the ignition delay. After the ignition, CH_2O quickly reacts, decreasing its concentration almost to zero. Thus, the expected CH_2O concentration during ignition process is three orders of magnitude higher than the detection limit of 5 ppm determined under the present experimental conditions. Taking into account that the decrease in the absorption coefficient of the spectral line center due to the collisional line broadening is compensated by the increased number density of formaldehyde molecules at elevated pressure, and that the relatively modest increase in temperature ($3\times$ compared to the experiments performed here) does not substantially change population distribution over the initial levels in the absorption transitions, it is reasonable to expect a similar detection limit at 30 bar and 900 K to that estimated here.

Thus, the experimental results presented above indicate that the sensitivity of our system is suitable for monitoring the expected CH_2O concentration during the ignition process with the required time resolution. We also point out that the relative CH_2O profiles can be obtained directly from the absorption spectrum, because pressure and temperature remain constant prior to the ignition moment. However, to derive absolute values of CH_2O concentrations, additional studies varying the temperature and pressure are needed for line assignment and to determine line broadening parameters. Furthermore, possible interferences from such species as CO , CO_2 [15], and H_2O [24] at expected concentrations of 0–2000 ppm (during preignition) also need to be quantified experimentally. These experiments are under way in our laboratory.

5 Summary

In this paper, we apply intracavity absorption spectroscopy for sensitive measurements of the absorption spectrum of formaldehyde in the spectral range from 6230 to 6420 cm^{-1} . The measurements are performed with a tunable broadband Er^{3+} -doped fiber laser. A sample of 1% CH_2O in air, made by the pyrolysis of the polymer POM, is placed inside the laser cavity. The spectral sensitivity of the measurements is controlled by the laser pulse duration. With 50- μs laser pulses, the sensitivity corresponds to an effective absorption path length of 45 m. The spectra recorded in our experiment reveal many new absorption lines of CH_2O . Some of them are five times stronger than the absorption lines recorded in the previous experiment [8] in a smaller spectral range (6351–6362 cm^{-1}). Therefore, monitoring of CH_2O with these strong absorption lines provides higher concentration sensitivity. The noise-equivalent detection limit of CH_2O , achieved with the strongest absorption line at 6252.64 cm^{-1} is estimated to be 5 ppm. If necessary, a detection limit below 1 ppm can be easily achieved with longer laser pulses.

High tolerance to broadband losses and the accessible time resolution of 50 μs make it possible to apply this detection system for time-resolved monitoring of CH_2O in harsh combustion environments, such as in combustion engines. Theoretical estimates of the temporal profiles of temperature and concentration of CH_2O after compression of a stoichiometric CH_4/air mixture indicate that the sensitivity achieved is sufficient for a corresponding experiment in an RCM. The Er^{3+} -doped fiber laser used in the experiment can also be applied for the detection of other combustion-relevant molecules such as CH_2O , CO , CO_2 , OH , H_2O , H_2S , NH_3 , C_2H_2 , and HCN [12]. In addition, the current experimental setup is well suited for time-resolved studies

of combustion processes in challenging environments such as flames, shock tubes, rapid compression machines, and combustion engines.

Acknowledgements We are thankful to H. Top and J. H. Marsman for their help in wet-chemical analysis and making formaldehyde.

References

1. D.I. Shin, T. Dreier, J. Wolfrum, Spatially resolved absolute concentration and fluorescence-lifetime determination of CH_2O in atmospheric-pressure CH_4/air flames. *Appl. Phys. B* **72**(2), 257–261 (2001)
2. J.E. Harrington, K.C. Smyth, Laser-induced fluorescence measurements of formaldehyde in a methane/air diffusion flame. *Chem. Phys. Lett.* **202**(3–4), 196–202 (1993)
3. A.J. Donkerbroek, A.P. van Vliet, L.M.T. Somers, P.J.M. Frijters, R.J.H. Klein-Douwel, N.J. Dam, W.L. Meerts, J.J. ter Meulen, Time- and space-resolved quantitative LIF measurements of formaldehyde in a heavy-duty diesel engine. *Combust. Flame* **157**(1), 155–166 (2010)
4. S. Wang, D.F. Davidson, R.K. Hanson, High-temperature laser absorption diagnostics for CH_2O and CH_3CHO and their application to shock tube kinetic studies. *Combust. Flame* **160**(10), 1930–1938 (2013)
5. A. Matsugi, H. Shiina, T. Oguchi, K. Takahashi, Time-resolved broadband cavity-enhanced absorption spectroscopy behind shock waves. *J. Phys. Chem A* **120**(13), 2070–2077 (2016)
6. P. Nau, J. Koppmann, A. Lackner, A. Brockhinke, Detection of formaldehyde in flames using UV and MIR absorption spectroscopy. *Z. Phys. Chem.* **229**(4), 483–494 (2015)
7. M. Staak, E.W. Gash, D.S. Venables, A.A. Ruth, The rotationally-resolved absorption spectrum of formaldehyde from 6547 to 6804 cm^{-1} . *J. Mol. Spectrosc.* **229**(1), 115–121 (2005)
8. W. Zhao, X. Gao, L. Deng, T. Huang, T. Wu, W. Zhang, Absorption spectroscopy of formaldehyde at 1.573 μm . *J. Quant. Spectrosc. Radiat. Transf.* **107**(2), 331–339 (2007)
9. V.M. Baev, T. Latz, P.E. Toschek, Laser intracavity absorption spectroscopy. *Appl. Phys. B* **69**(3), 171–202 (1999)
10. I. Rahinov, A. Goldman, S. Cheskis, Intracavity laser absorption spectroscopy and cavity ring-down spectroscopy in low-pressure flames. *Appl. Phys. B* **81**(1), 143–149 (2005)
11. J. Sierks, T. Latz, V.M. Baev, P.E. Toschek, Proceedings of the 1996 European Quantum Electronics Conference (EQEC'96), 8–13 September 1996, Hamburg, p. 100, QWB6
12. B. Löhden, S. Kuznetsova, K. Sengstock, V.M. Baev, A. Goldman, S. Cheskis, B. Pálsdóttir, Fiber laser intracavity absorption spectroscopy for in situ multicomponent gas analysis in the atmosphere and combustion environments. *Appl. Phys. B* **102**(2), 331–344 (2011)
13. F. Stoeckel, M.D. Schuh, N. Goldstein, G.H. Atkinson, Time-resolved intracavity laser spectroscopy: 266 nm photodissociation of acetaldehyde vapor to form HCO. *Chem. Phys.* **95**(1), 135–144 (1985)
14. P. Sheehy, J.I. Steinfeld, Discharge-flow kinetics measurements using intracavity laser absorption spectroscopy. *J. Phys. Chem. B* **109**(17), 8358–8362 (2005)
15. A. Fomin, T. Zavlev, I. Rahinov, S. Cheskis, A fiber laser intracavity absorption spectroscopy (FLICAS) sensor for simultaneous measurements of CO and CO_2 concentrations and temperature. *Sens. Actuators B* **210**, 431–438 (2015)
16. P. Fjodorow, M. Fikri, C. Schulz, O. Hellmig, V.M. Baev, Time-resolved detection of temperature, concentration, and pressure in a shock tube by intracavity absorption spectroscopy. *Appl. Phys. B* **122**, 159 (2016)
17. P. Fjodorow, I. Baev, O. Hellmig, K. Sengstock, V.M. Baev, Sensitive, time-resolved, broadband spectroscopy of single transient processes. *Appl. Phys. B* **120**(4), 667–673 (2015)
18. J. Hünkemeier, R. Böhm, V.M. Baev, P.E. Toschek, Spectral dynamics of multimode Nd^{3+} - and Yb^{3+} -doped fibre lasers with intracavity absorption. *Opt. Commun.* **176**(4–6), 417–428 (2000)
19. L.S. Rothman, I.E. Gordon, Y. Babikov, A. Barbe, D. Chris Benner, P.F. Bernath, M. Birk, L. Bizzocchi, V. Boudon, L.R. Brown, A. Campargue, K. Chance, E.A. Cohen, L.H. Coudert, V.M. Devi, B.J. Drouin, A. Fayt, J.-M. Flaud, R.R. Gamache, J.J. Harrison, J.-M. Hartmann, C. Hill, J.T. Hodges, D. Jacquemart, A. Jolly, J. Lamouroux, R.J. LeRoy, G. Li, D.A. Long, O.M. Lyulin, C.J. Mackie, S.T. Massie, S. Mikhailenko, H.S.P. Müller, O.V. Naumenko, A.V. Nikitin, J. Orphal, V. Perevalov, A. Perrin, E.R. Polovtseva, C. Richard, M.A.H. Smith, E. Starikova, K. Sung, S. Tashkun, J. Tennyson, G.C. Toon, V.G. Tyuterev, G. Wagner, The HITRAN2012 molecular spectroscopic database. *J. Quant. Spectrosc. Radiat. Transf.* **130**, 4–50 (2013)
20. J.G. Boyles, S. Toby, The mechanism of the polymerization of gaseous formaldehyde. *J. Polym. Sci. C* **4**(6), 411–415 (1966)
21. M. Day, J.D. Cooney, C. Touchette-Barrette, S.E. Sheehan, Pyrolysis of mixed plastics used in the electronics industry. *J. Anal. Appl. Pyrolysis* **52**, 199–224 (1999)
22. D.G. Goodwin, H.K. Moffat, R.L. Speth, (2015). Cantera: an object-oriented software toolkit for chemical kinetics, thermodynamics, and transport processes. Version 2.2.0 [Data set]. Zenodo. <http://doi.org/10.5281/zenodo.48735>
23. G.P. Smith, D.M. Golden, M. Frenklach, N.W. Moriarty, B. Eiteeneer, M. Goldenberg, C.T. Bowman, R.K. Hanson, S. Song, W.C. Gardiner, J.V.V. Lissanski, Z. Qin, n.d. GRI-MECH 3.0 [WWW Document]. http://www.me.berkeley.edu/gri_mech/
24. A. Fomin, T. Zavlev, I. Rahinov, V.A. Alekseev, A.A. Konnov, V.M. Baev, S. Cheskis, Fiber laser intracavity spectroscopy of hot water for temperature and concentration measurements. *Appl. Phys. B* **121**, 345–351 (2015)